Effects of Electron Correlation and Spin Projection on Rotational Barriers of Trithiocarbenium Ion $[C(SH)_3]^+$ and Radical Dication $[C(SH)_3]^{\cdot,2+}$

RAINER GLASER,[1] GRACE SHIAHUY CHEN,[1] HANSJÖRG GRÜTZMACHER[2]

[1] *Department of Chemistry, University of Missouri–Columbia, Columbia, Missouri 65211*

[2] *Institut für Anorganische Chemie, Eidgenössische Technische Hochschule, CH-8092 Zürich, Switzerland*

Received 19 July 1996; accepted 14 October 1996

ABSTRACT: Theoretical level dependencies are discussed of relative isomer stabilities and rotational barriers of trithiomethyl cation $[C(SH)_3]^+$ (**a**) and of radical dication $[C(SH_3)]^{\cdot,2+}$ (**b**). Spin polarization and dynamic electron correlation are very important for the radical dictation. Removal of an electron from one of the degenerate π-HOMOs of C_{3h} symmetric $[C(SH)_3]^+$ stabilizes the remaining π electron to such an extent that the unpaired electron is not in the HOMO of the dictation. The radial π MO's ''diving below the Fermi level'' facilitates strong spin polarization because of its energetic proximity to σ MOs. Projection of the first three higher spin states eliminates spin contaminations, and the terms E(PUHF(s + 3))-E(UHF) and E(PMP4(s + 3))-E(MP4) are discussed. The combination of annihilation of spin contamination and electron correlation is essential for the determination of relative energies and rotational barriers of the radical dication. The results obtained at this level match the results of high level QCISD(T) calculations in a near-quantitative fashion. Perturbation theory alone does not correct for spin contamination even if it is carried to full fourth order and includes triple excitations; the E(PMP4(s + 3))-E(MP4) values are all negative and can exceed 5 kcal/mol in magnitude. Previous studies showed that annihilation of spin contaminations is important in regions of potential energy surfaces where σ bonds are broken (homolytic dissociation), formed (radical addition), or both (H abstraction by radical). Our findings stress that the annihilation of spin contaminations can be just as

Dedicated to Prof. Andrew Streitwieser on the occasion of his 70th birthday.

Correspondence to: R. Glaser; e-mail: chemrg@showme.missouri.edu

Contract grant sponsor: NATO

CCC 0192-8651 / 97 / 081023-13

important for any process that greatly alters spin polarization and even if that process proceeds without breaking or forming of σ bonds. For comparison, density functional theory also was employed in the potential energy surface analyses. The results obtained with the B3LYP formalism were found to be less susceptible to spin contamination and resulted in rather good agreement with the best pertubation and configuration interaction results. *J Comput Chem* **18**: 1023–1035, 1997

Keywords: relative isomer stabilities; rotational barriers; thiomethyl cation; radical dication; electron correlation; spin projection

Introduction

Sulfur is effective at stabilizing polycations[1] due to its low ionization potential and electronegativity.[2] Thiocarbenium ions[3] were prepared and characterized[4–6] and some of these are stable in the solid state. X-ray crystal structures of several di-[7] and trithiosubstituted[8] carbenium ions were obtained. In a recent study that combined experimental and *ab initio* computational investigations of the systems $[CH_n(XR)_{3-n}]^+$[X = O, S, Se, Te; R(exp.) = 2, 4, 6-*i* $Pr_3C_6H_2$, R(calcd.) = H; n = 0–2], we found that the mode of stabilization by sulfur and the heavier homologs differs greatly from the mechanism of stabilization of carbenium ions by oxygen.[9] These studies indicated an enhanced charge separation in $[C(OH)_3]^+$ instead of the commonly expected charge delocalization. For $[C(OH)_3]^+$, natural population analysis (NPA) suggested a positive charge on carbon that is larger than unity (+1.3). The homologous ions $[C(XH)_3]^+$ (X = S, Se, Te) were found to differ fundamentally in that the carbon center is negatively charged as the result of effective X → C donation in the σ and π systems. In a subsequent study, we explored the possibility of further oxidation for the sulfur system via *ab initio* potential energy surface analysis of $[C(SH)_3]^+$ and of the radical dication $[C(SH)_3]^{\cdot,2+}$.[10] The electronic features suggested by the NPA analysis for the monocation were fully corroborated by topological analysis of the electron density distributions in Cartesian space. Moreover, it was found that this unexpected electronic motif persists even in the dication. Oxidation of the monocation primarily removes sulfur π-electron density and removes only some electron density from the central C atom. The α-excess spin density is entirely concentrated on S atoms and the carbon carries some β-spin density because of spin polarization. Minima and transition state structures for isomerization were reported for $[C(SH)_3]^+$ and $[C(SH)_3]^{\cdot,2+}$ and (P)MP4(full, sdtq)/ 6–31G*// HF/ 6–31G* + ΔVZPE(RHF/6–31G*) level activation barriers to rotation were discussed as probes for the importance of conjugation.[11]

With the present study we expand on one aspect of our studies of the cations $[C(SH)_3]^{n+}$ that is of more general theoretical interest, and this aspect concerns the energetic effects of annihilation of unwanted spin contaminations in the wave functions of the radical $[C(SH)_3]^{\cdot,2+}$ at the Hartree–Fock (HF) and Møller–Plesset (MP) levels. In 1986 Schlegel combined unrestricted fourth-order perturbation theory with spin projection (PMP4) to annihilate the largest spin contaminant,[12] and the methodology for full annihilation was developed shortly thereafter.[13] Homolytic dissociations were studied and approximate and complete annihilation gave PMP4 potential energy curves that agreed well with very accurate configuration interaction (CI) calculations. The potential energy surface characteristics can be affected significantly in regions where spin contamination becomes important and especially when electron correlation corrections are treated by MP perturbation theory. In one study of the addition of an H atom to ethyne, ethene, and formaldehyde, the effects of spin contamination on both geometries and activation barriers were studied at the PMP2 level. The PMP2 data provided a great improvement over the MP2 level and closely approximated the PMP4 results.[14] Studies of radical additions to simple unsaturated compounds[15–17] showed that good agreement with an experiment can be obtained when corrections for spin projection are combined with electron correlation corrections while the barrier heights generally were too high when spin contamination was ignored. Subsequent studies (Table I) of the addition of ethene radical cation to ethene,[18] of the additions of *tert*-butyl radical and benzyl radical to ethene,[19] and of the addition of simple σ radicals to mono- and difluoroethene[20] corroborated

TABLE I.
Development and Applications of Spin Projected Møller–Plesset Perturbation Theory.

Method	Systems Studied	Authors, Year
PMP4, PA of SC	Diss. of LiH of HF	Schlegel, 1986[12]
PMP4, CA of SC	Diss. of LiH, HF, and H_2O	Schlegel, 1988[13]
PMP2 structures	Add. of $H^{\cdot}$ to C_2H_2, C_2H_4 & H_2CO	McDouall & Schlegel, 1989[14]
PMP4, PA of SC	Add. of $HO^{\cdot}$ to C_2H_2 & C_2H_4	Sosa & Schlegel, 1987[15]
PMP4, PA of SC	Add. of $H^{\cdot}$ to C_2H_4 & H_2CO	Sosa & Schlegel, 1986[16]
PMP4, PA of SC	Add. of $Me^{\cdot}$ to C_2H_4 & H_2CO	Gonzalez et al., 1989[17]
PMP4, CA of SC	H abstr. from CH_4 by $H^{\cdot}$, $HO^{\cdot}$, or O_3	Gonzalez et al., 1990[22]
PMP4, PA of SC	^2N and ^4N reactions with $Me^{\cdot}$	Gonzalez & Schlegel, 1992[26]
PMP4, PA of SC	H abstr. from HXCO (X = H, F, Cl) by $HO^{\cdot}$	Francisco, 1992[23]
PMP4, CA of SC	Add. of $C_4H_4^{\cdot+}$ to C_2H_4	Alvarez–Idaboy et al., 1993[18]
PMP4, PA of SC	H abstr. from NH_3 by $HO^{\cdot}$	Corchado et al., 1993[24]
PMP4, CA of SC	Add. of tert-$C_4H_9^{\cdot}$ and $Bz^{\cdot}$ to C_2H_4	Arnaud et al., 1994[19]
PMP4, CA of SC	Add. of σ radicals to fluoroethene	Donovan & Famini, 1994[20]
PMP4, PA of SC	Add. of bicyclo [2,1,0]pentyl radical	Bach et al., 1994[27]
PMP2, PA of SC	Add of $R^{\cdot}$ to alkenes	Wong & Radom, 1995[21]
PMP4, CA of SC	H abstr. from chloroethane by $HO^{\cdot}$	Sekusak et al., 1995[25]

[a] Spin projected fourth-order Møller–Plesset theory (PMP4) with partial (PA) or complete annihilation (CA) of spin contaminants (SC).

that the energetics of the radical addition reactions can be very sensitive to electron correlation and spin contamination. Recent theoretical model dependencies of some prototypical radical addition reactions further emphasize this point.[21] While the thermochemistry of the reactions shows moderate theoretical level dependency, significant differences of up to 10 kcal/mol were found between activation barriers computed with and without annihilation of spin contaminations. Importantly, the work of Alvarez–Idaboy et al.[18] shows that elimination of spin contaminants can *increase* the activation barriers while in most cases a *decrease* of activation barriers is observed. The study by Donovan and Famini[20] is important because it shows that the predicted regiochemistry can depend on whether the annihilation of spin contaminants was or was not combined with a perturbational electron correlation treatment. Similar methodological effects were reported for H-abstraction reactions from methane,[22] from HXCO (X = H, F, Cl),[23] from ammonia,[24] and from chloroethane.[25] In the study by Covchado et al.,[24] for example, it was pointed out that the spin projection had larger effects on the kinetic barrier than on the reaction thermochemistry and the PMP4 calculations provided activation barriers for H transfer that agree well with the experiments. These same conclusions are true for other H-abstraction reactions and for the insertion reaction as well.[26] Yet, there are again some notable exceptions. Recently, Bach et al. studied the properties of the radical obtained by H abstraction from bicyclo-[2.1.0]pentane and its reactions (H abstraction, $HO^{\cdot}$ addition) at the MP4 level without and with annihilation of spin contamination. The activation barriers determined at the MP4 and PMP4 levels differed only very slightly.[27]

All of these studies of annihilation of spin contaminations (*vide supra*) can be summarized by stating that spin projection becomes important in regions of the potential energy surfaces where σ bonds are broken (homolytic dissociation), formed (radical addition), or both (H abstraction). Because the annihilation of spin contaminants reduces spin polarization,[28] one would expect the largest effects in the transition regions because these regions are characterized by the most spin decoupling and therefore are prone to realize strong spin polarization. We have been interested in spin density distributions and recently reported a study on the rotational automerization of allyl radical.[28b] It was found that spin projection was necessary to predict the correct transition state structure. Only when perturbational corrections to electron correlation were combined with annihilation of spin contamination did the predicted activation barrier for rotational automerization agree with high level CI data and with the experiment. Our study of allyl radical shows that the effects of spin contamination can be significant even in processes in which

no σ bonds are broken and where the electronic reorganization merely involves the breaking of π-dative bonds and spin localization. This conclusion is corroborated by other studies of the allyl radical[29] as well as the studies of the benzyl radical.[30] Here, we present a comparative analysis of relative isomer stabilities and of rotational barriers of $[C(SH)_3]^+$ and $[C(SH)_3]^{\cdot,2+}$. This analysis has several attractive features to add to this discussion. The theoretical level affects the monocation characteristics only slightly and this system provides a good point of reference. A most pertinent advantage relates to the fact that dynamic electron correlation becomes particularly important for the radical dication. It is known that dynamic electron correlation between π and σ electrons is critical in molecules with charged π systems,[31] and this is even more true for the dication for the following reason. Removal of one electron from one of the degenerate π highest occupied molecular orbitals (HOMOs) of $[C(SH)_3]^+$ stabilizes the remaining π electron greatly and the MO of the unpaired π-radical is *not* the HOMO in the dication. The unpaired π MOs ''diving below the Fermi level'' facilitates strong spin polarization because of its energetic proximity to σ MOs. It is for this scenario that energetic effects of spin contamination and its annihilation should be particularly pronounced, even though no σ bonds are broken or formed. It will be shown that the combination of annihilation of spin contamination and electron correlation is essential for the determination of relative isomer stabilities and for activation barriers. At this level, the results of the perturbation calculations match high level QCIS(T) data in near-quantitative fashion. Quadratic CI theory is much less sensitive to spin contamination and thus can serve as the standard for the assessment of the accuracy of the perturbation results. Much less is known about the reliability of density functional theory (DFT) in such cases, and we present results of semiempirical solutions for comparison.

Theory and Computations

Restricted (RHF) and unrestricted (UHF) Hartree–Fock or HF theory[32] were employed for the closed- and open-shell systems, respectively. While the wave functions obtained with the UHF formalism are eigenfunctions of the Hamiltonian and the S_z operators,[33] they are not eigenfunctions of the S^2 operator. As a result, the wave functions of the doublet systems are spin contaminated to some extent by admixtures of quartet, sextet, and higher spin states.[34,35] The eigenvalues of the S^2 operator are given as a measure of the spin contamination. Because the projection operator commutes with the charge density operator,[36] the electron density remains unaffected by the projection and effects of spin contamination on the optimized structures are expected to be small.[28] Complete gradient optimizations of geometries and vibrational analysis were carried out at the HF/6–31G* level as described previously.[10] The zero-point energies calculated at the HF level were scaled in the usual fashion[37] (factor 0.9) when applied to relative energies. Electron correlation effects on relative stabilities were estimated using full fourth-order MP perturbation theory [MP4(full, sdtq)/6–31G*//HF/6–31G*]. Borden and Davidson stressed the importance of triple excitations to correctly compute molecules with charged π systems.[31] The work by Knowles and Handy[38] points out that spin contamination adversely affects the convergence of the perturbation series and that a significant improvement can be obtained after spin projection. To probe these energetic consequences of spin contamination, we also determined the HF and MP4 energies after annihilation. QCI theory[39] with all single and double excitations considered and including a perturbation correction for triple excitations, QCISD(T), is used as the high level standard in the assessment of the performances of all other methods. DFT[40] has emerged in recent years as one of the more promising approaches within the arsenal of semiempirical methods and we have included the results of B3LYP[41] calculations for comparison. In Table II we report the results of the potential energy surface exploration at the HF level and higher level energies determined with the HF/6–31G* structures. The results of computations that involved the annihilation of spin contaminants are listed in Table III. The energies PUHF(s + 1) and PUHF(s + 3) were obtained after removal of the next higher spin contamination (quartet) and after removal of the spin contaminations associated with the first three higher spin states (s + 1 to s + 3) Projection of just the next higher spin state results in S^2 eigenvalues of 0.750 ± 0.001 and only for **1b** and **2b** the S^2 values of 0.750 ± 0.060 remain slightly higher. Annihilation of the first higher spin state removes the major part of the spin contamination successfully as indicated by the S^2 eigenvalues after projection of the quartet state.[42,43] Projection of the first three

TABLE II.
Total and Vibrational Zero-Point Energies.

Molecule	Sym.	HF/6−31G* Energy	HF/6−31G* VZPE	HF/6−31G* NIMAG	MP4(sdtq) Energy	B3LYP Energy	QCISD(T) Energy
$C(SH)_3^+$, **1a**	C_{3h}	−1231.854177	24.27	0	−1232.450046	−1234.174283	−1232.450180
$C(SH)_3^{2+}$, **1b**	C_{3h}	−1231.319016	23.16	0	−1231.888288	−1233.608296	−1231.898812
$C(SH)_3^{2+}$, **1b′**	C_s	−1231.319912	23.19	0	−1231.890024	−1233.609855	−1231.900278
$C(SH)_3^+$, **2a**	C_s	−1231.850775	24.16	0	−1232.446974	−1234.171133	−1232.447104
$C(SH)_3^{2+}$, **2b**	C_s	−1231.321188	23.28	0	−1231.891893	−1233.610912	−1231.901983
$C(SH)_3^{2+}$, **3b-c1**	C_1	−1231.240092	23.86	0	−1231.827837	−1233.544650	−1231.830816
$C(SH)_3^{2+}$, **3b-c2**	C_1	−1231.243485	24.18	0	−1231.830563	−1233.546176	−1231.833077
$C(SH)_3^{2+}$, **3b-t1**	C_1	−1231.245134	24.07	0	−1231.831865	−1233.547899	−1231.834497
$C(SH)_3^{2+}$, **3b-t2**	C_1	−1231.245215	24.10	0	−1231.831733	−1233.548147	−1231.834548
$C(SH)_3^+$, **4a**	C_1	−1231.837539	23.89	1	−1232.434893	−1234.157807	−1232.435292
$C(SH)_3^{2+}$, **4b**	C_1	−1231.310806	23.01	1	−1231.892639	−1233.601374	−1231.894806
$C(SH)_3^+$, **5a-u**	C_S	−1231.835657	23.96	1	−1232.433210	−1234.156099	−1232.433562
$C(SH)_3^+$, **5a-w**	C_S	−1231.836563	23.84	1	−1232.434070	−1234.156970	−1232.434513
$C(SH)_3^{2+}$, **5b-u**	C_S	−1231.313212	23.10	1	−1231.894728	−1233.600774	−1231.895788
$C(SH)_3^{2+}$, **5b-w**	C_S	−1231.305256	22.95	1	−1231.889498	−1233.598623	−1230.891268

Energies in atomic units. RHF/6−31G* for closed shell systems and UHF/6−31G* for open shell systems. MP4(sdtq) and QCISD(T) calculations included all electrons in the active space. The MP4(sdtq), QCISD(T),and B3LYP calculations employed the 6−31G* basis set and were based on the HF/6−31G* structures. Vibrational zero-point energies (VZPE) in kcal/mol as calculated. NIMAG, number of imaginary frequencies. S^2 eigenvalues of UHF wave functions: **1b**, 1.1431; **1b**, 1.1410; **2b**, 1.1120; **3b-c1**, 0.7766; **3b-c2**, 1.1761; **3b-t1**, 0.7734; **3b-t2**, 0.7770; **4b**, 0.7883; **5b-u**, 0.7630; **5b-w**, 0.7631.

TABLE III.
Results of Calculations Involving Annihilation of Spin Contamination.

Molecule	PUHF(s + 1) Energy	ΔE_1	PUHF(s + 3) Energy	ΔE_2	PMP4(s + 3) Energy	ΔE_3
$C(SH)_3^{2+}$, **1b**	−1231.336728	−11.11	−1231.335311	0.89	−1231.900634	−7.75
$C(SH)_3^{2+}$, **1b**	−1231.337373	−10.96	−1231.335983	0.87	−1231.902175	−7.62
$C(SH)_3^{2+}$, **2b**	−1231.338129	−10.63	−1231.336884	0.78	−1231.903563	−7.32
$C(SH)_3^{2+}$, **3b-c1**	−1231.245042	−3.11	−1231.245000	0.03	−1231.829719	−1.18
$C(SH)_3^{2+}$, **3b-c2**	−1231.248346	−3.05	−1231.248316	0.02	−1231.832228	−1.04
$C(SH)_3^{2+}$, **3b-t1**	−1231.249867	−2.97	−1231.249837	0.02	−1231.833493	−1.02
$C(SH)_3^{2+}$, **3b-t2**	−1231.250162	−3.10	−1231.250123	0.02	−1231.833631	−1.19
$C(SH)_3^{2+}$, **4b**	−1231.315029	−2.65	−1231.317971	0.04	−1231.895114	−1.55
$C(SH)_3^{2+}$, **5b-u**	−1231.316630	−2.14	−1231.316623	0.00	−1231.895847	−0.70
$C(SH)_3^{2+}$, **5b-w**	−1231.308672	−2.14	−1231.308665	0.00	−1231.890627	−0.71

Energies in atomic units. ΔE values in kcal/mol.

TABLE IV.
Relative Energies.

Parameter	HF No Proj.	ΔVZPE Scaled	PUHF Proj. s + 1	PUHF Proj. s + 3	MP4 No. Proj.	PMP4 Proj. s + 3	DFT B3LYP	QCISD(T)
I-Pref (**1b**′ over **1b**)	0.56	−0.03	0.40	0.42	1.09	0.97	0.98	0.92
I-Pref (**1a** over **2a**)	2.13	−0.10			1.93		1.98	1.93
I-Pref (**1b** over **2b**)	−1.36	0.11	−0.88	−0.99	−2.26	−1.84	−1.64	−1.99
I-Pref (**3b-t2** over **3b-t1**)	0.05	−0.03	0.19	0.18	−0.08	0.09	0.16	0.03
I-Pref (**3b-t2** over **3b-c2**)	1.09	0.07	1.14	1.13	0.73	0.88	1.24	0.92
I-Pref (**3b-c2** over **3b-c1**)	2.13	−0.29	2.07	2.08	1.71	1.57	0.96	1.42
I-Pref (**1b** over **3b-t2**)	46.31	0.85	54.32	53.46	35.49	42.05	37.74	40.33
E_A(**1a** ⇒ **4a**)	10.44	−0.34			9.51		10.34	9.34
E_A(**1b** ⇒ **4b**)	5.15	−0.13	13.62	12.76	−2.73	3.46	4.34	2.51
E_A(**2a** ⇒ **4a**)	8.31	−0.24			7.58		8.36	7.41
E_A(**2b** ⇒ **4b**)	6.51	−0.24	14.50	13.75	−0.47	5.30	5.99	4.50
E_A(**2a** ⇒ **5a-u**)	9.49	−0.18			8.64		9.43	8.50
E_A(**2a** ⇒ **5a-w**)	8.92	−0.29			8.10		8.89	7.90
E_A(**2b** ⇒ **5b-u**)	5.01	−0.16	13.49	12.71	−1.78	4.84	6.36	3.89
E_A(**2b** ⇒ **5b-w**)	10.00	−0.30	18.48	17.71	1.50	8.12	7.71	6.72

Isomer preference energies (I-Pref), activation energies (E_A), ionization energies (IE), and hydride affinities (HA) in kcal / mol. ΔVZPE terms calculated at the HF level are scaled (factor 0.9), and they are to be added to the relative energies.

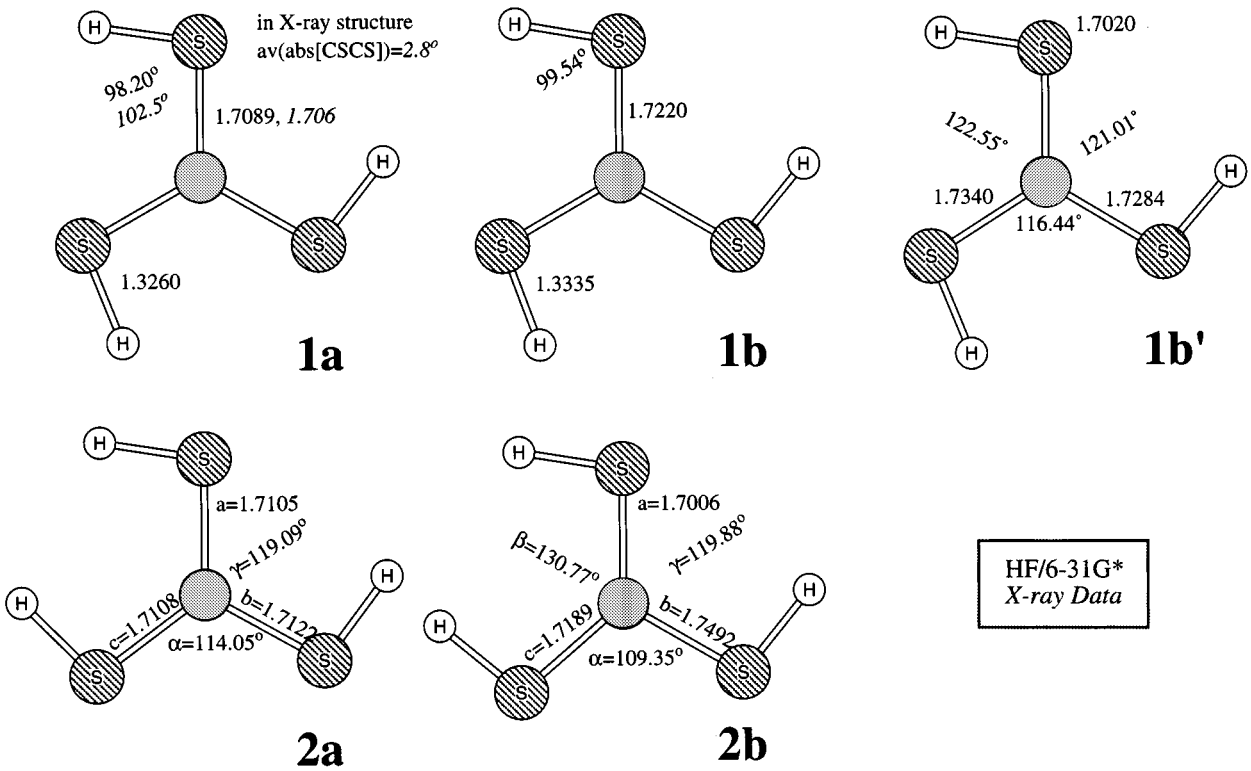

FIGURE 1. Structures of the minima C_{3h}-**1a** and C_s-**2a** of $[C(SH)_3]^+$. Structures **1b** (C_{3h}) and **1b**′ (C_S) are minima of dication $[C(SH)_3]^{\cdot,2+}$ resulting by oxidation of C_{3h}-**1a**. Dication C_s-**2b** is the oxidation product of **2a**. Values given in italics for **1a** are the average X-ray data for $[C(SR)_3]^+$ with R = 2,4,6-tri-(isopropyl)phenyl.

unwanted spin states results effectively in complete annihilation. Pertinent relative energies obtained without and with annihilation at the HF and MP4 levels as well as at the DFT and QCI levels are summarized in Table IV. Calculations were performed with the program Gaussian 94[44] and earlier versions on a network of IBM/RS-6000, Silicon Graphics Indigo, and PowerChallenge L computers.

Results and Discussion

EQUILIBRIUM STRUCTURES AND ISOMERIZATIONS OF $[C(SH)_3]^+$ AND $[C(SH)_3]^{\cdot,2+}$

An analysis of the potential energy surfaces of $[C(SH)_3]^+$ and $[C(SH)_3]^{\cdot,2+}$ was given previously[10] and we briefly review the relevant parts. Isomeric structures are distinguished by numbers and the labels **a** and **b** are used to denote the cation and the dication, respectively. Unless otherwise noted, relative energies in the following refer to the highest level of perturbation theory, PMP4(full, sdtq)/6−31G*//HF/6−31G* + ΔVZPE (HF/6−31G*).

The C_{3h} structures **1a** and **1b** are minima (Fig. 1). The X-ray structure of $[C(SR)_3]^+$ with R = 2,4,6-tri(isopropyl)phenyl realizes *de facto* C_{3h} symmetry of the central unit and the C—S bond lengths agree well with the calculated structure **1a**. The wave function for **1b** is asymmetric and allows for reduction in molecular symmetry. Optimization within C_s symmetry leads to the Jahn−Teller distorted structure **1b′**, which is preferred over **1b** by less than 1 kcal/mol. **1b′** is modestly distorted in that two C—S bonds are elongated while one is shortened. The distorted structure **1b″** in which one C—S bond is elongated while the two other are shortened corresponds to the transition state structure for pseudorotation.[45] The rather similar energies of **1b** and **1b′** indicate that the pseudorotation of **1b′** is essentially unhindred and there is no need to optimize **1b″**. Rotation about one of the C—S bonds in **1** leads to structures **2** and the C_s structures **2a** and **2b** are minima. While **1a** is preferred over **2a**, the dication **1b** is less stable than **2b**. Several distonic stereoisomers with S—S bonds were located (Fig. 2). In **3b-c1** and **3b-c2**, the endocyclic S—H bonds are cis with regard to each other, while the endocyclic S—H bonds are trans to each other in **3b-t1** and **3b-t2**. Isomers **3b-t2** and **3b-t1** are nearly isoenergetic and the cis structures are more stable than the trans structures. All of the isomers of **3b** are more than 35 kcal/mol less stable than C_{3h}-**1b**. The isomerization between **2** and **1** involves rotation about the c bond of **2** indicated in Figure 1 and involves the chiral transition state structures **4a** and **4b**. Rotation about the a or b bonds in **2a** or **2b** results in automerization via the C_s-symmetric transition state structures **5a** and **5b** (Fig. 3). The structures **5** come as isomers **5-w** and **5-u**, depending on whether rotation occurs about the a or the b bond, respectively. The labels w and u describe the shape of the in-plane H—S—C—S—H fragment.

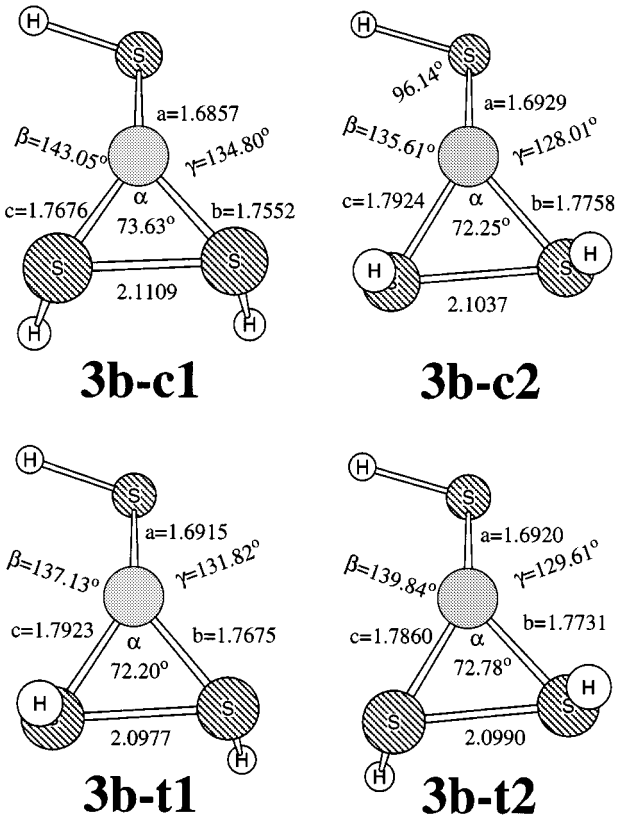

FIGURE 2. Stereoisomers **3b** are local minima of the radical dication $[C(SH)_3]^{\cdot,2+}$.

MO DIAGRAMS OF RADICAL DICATIONS

The valence-MO diagrams of **1a** and of the oxidized species **1b** and **1b′** are shown in Figure 4. The RHF MO levels are shown for **1a** and for the radicals set of α- and β-spin orbitals are shown. With the exception of π_{28} of the dication, all of the MOs are occupied but, for the sake of clarity, only the π electrons are indicated by ↑ (α spin) and ↓ (β spin).

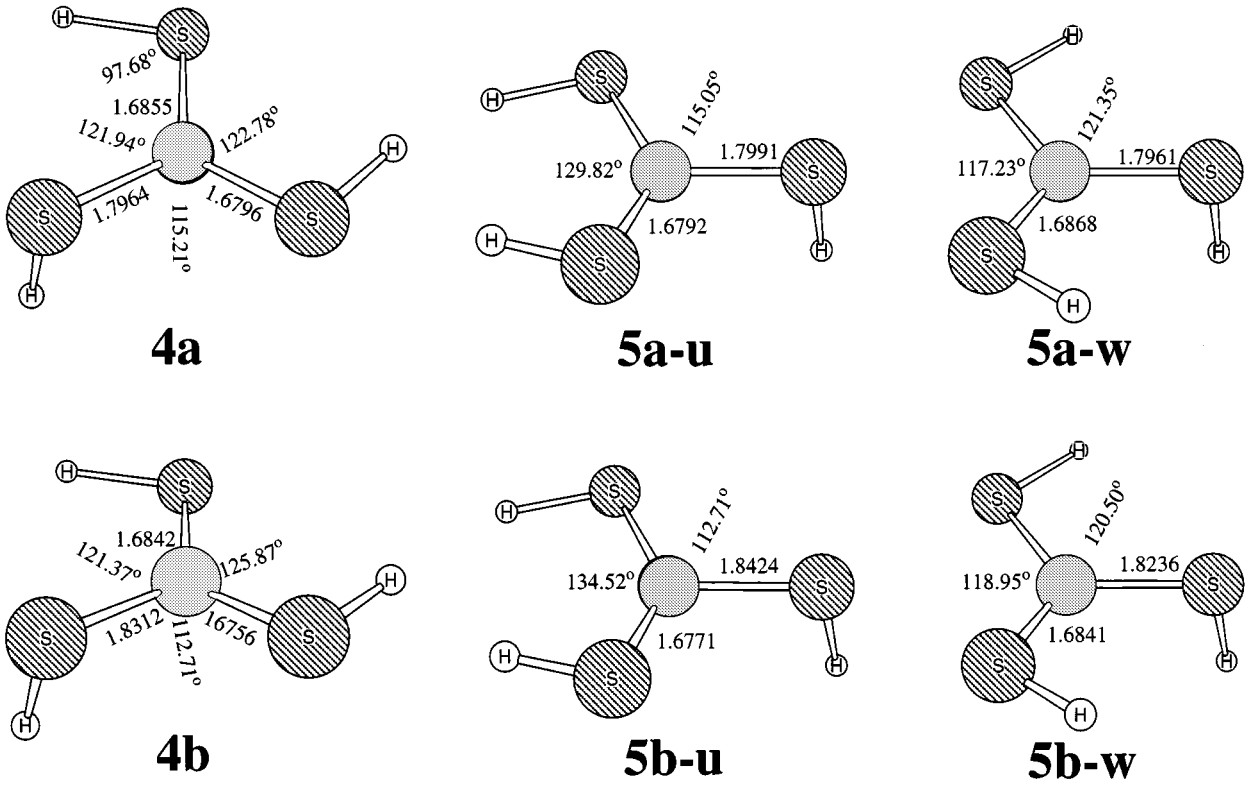

FIGURE 3. The transition state structures for isomerization **1** ⇒ **4**‡ ⇒ **2** and automerizations **2** ⇒ **5-u**‡ ⇒ **2** and **2** ⇒ **5-w**‡ ⇒ **2** are shown for the monocation (top) and the dication (bottom).

Chemists are inclined to assume that the oxidation of a closed-shell system leads to an open-shell system in which the unpaired electron resides in the HOMO. This assumption, of course, reflects an education in MO theory that for several decades used to focus on Hückel theory. Removal of one electron from the degenerate π HOMO ($\pi_{27/28}$) results in a stabilization of the remaining unpaired π electron (α-π_{26}) significantly below the energy of the remaining quasidegenerate π HOMO (α-π_{28} and β-π_{27}) of the radical dication. The energies of the electrons of the all-bonding π_{23} MO in **1a** become greatly different in the dication (α-π_{23} and β-π_{24}). While the lowering of the MO of the unpaired electron below the energy of the remaining doubly occupied MO of the formerly degenerate HOMO set, although hardly ever recognized, can be rationalized as a consequence of a reduction of electron–electron repulsion, it is most intriguing indeed that sets of spin paired π *and* σ electrons are both higher in energy compared to the MO associated with the unpaired π radical. Dynamic electron correlation becomes so important in this charged π radical because of this readily identifiable feature of the MOs.

ENERGETIC EFFECTS OF ANNIHILATION OF SPIN CONTAMINATIONS AND OF ELECTRON CORRELATION

The energetic effects of annihilation of spin contaminations and of electron correlation are conveniently discussed with the parameters ΔE included in Table III. The energy differences $\Delta E_1 = E(\text{PUHF(s + 1)}) - E(\text{UHF})$ and $\Delta E_2 = E(\text{PUHF(s + 3)}) - E(\text{PUHF(s + 1)})$ allow for an appreciation of partial and complete annihilation of spin contamination at the HF level. Effects of spin annihilation at the electron correlated level were assessed via $\Delta E_3 = E(\text{PMP4(s + 3)}) - E(\text{MP4})$ and only complete annihilation was considered in this case. A positive ΔE means that decontamination increases the energy. As can be seen from Table III, the energy differences ΔE_1 are substantial and range from +5 to −10 kcal/mol. The ΔE_2 values are all positive and are generally small. Because

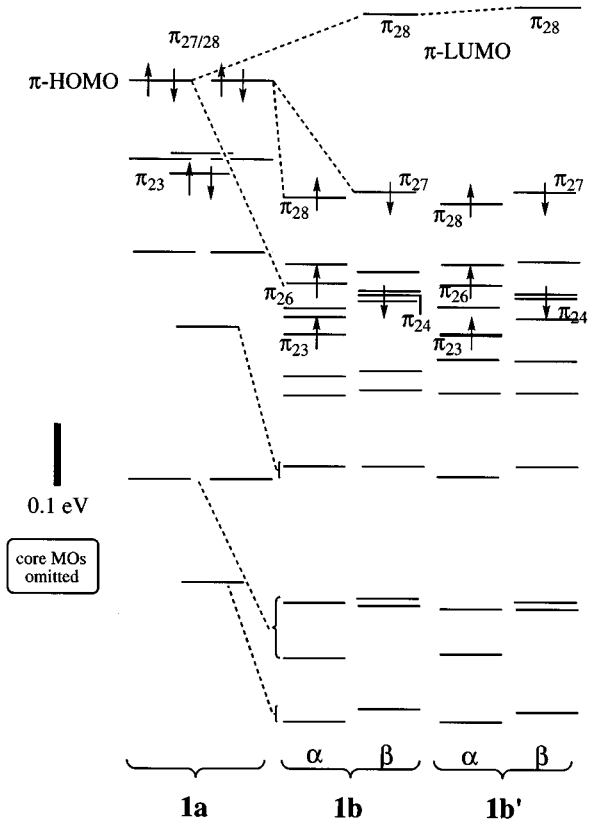

FIGURE 4. The MO diagrams for **1a**, **1b**, and **1b**′ are drawn to scale.

the contaminations are completely eliminated after projection of the first three higher spin states, we report the PMP4(s + 3) energies together with the ΔE_3 values. The ΔE_3 values all are negative; that is, the PMP4 energies are lower than the MP4 energies throughout; and the magnitudes of ΔE_3 are large for most of the open structures while being modest for the ring structures.

An example for significant deviation between MP4 and PMP4 data relates to the relative isomer preference between **1b** and the distonic structures **3b**. As can be seen from the ΔE_i values in Table III, the effects of spin projection are similar and small for all isomers of **3b**. Not so for **1b**. The annihilation of spin contaminations increases the PUHF value of I-Pref (**1b** over **3b**–**t2**) by nearly 10 kcal/mol. Electron correlation affects this value in the opposite direction and more, such that the PMP4 value becomes 42.1 kcal/mol. The MP4 value is about 6.5 kcal/mol lower still because the energy increase associated with proper spin annihilation is not accounted for.

The energetic consequences of annihilation of spin contaminations and/or of electron correlation on relative stabilities of isomers **1** and **2** and on rotational barriers are demonstrated in a compelling fashion with the graphical representations of the potential energy surfaces of $[C(SH)_3]^+$ and $[C(SH)_3]^{\cdot,2+}$ shown in Figure 5. In the top left in Figure 5, the potential energy diagram is represented as computed at the HF/6–31G* + ΔVZPE level and energetic consequences of either annihilation of spin contamination or of electron correlation are shown in the lower left and the upper right, respectively. On the bottom right are shown the energetics obtained after annihilation *and* electron correlation at the PMP4/ 6–31G*// HF/ 6–31G* + ΔVZPE level. In Figure 6 the results of the DFT and QCISD(T) calculations are presented in exactly the same manner as with Figure 5. It is immediately obvious that the best perturbation theoretical data agree in a near-quantitative fashion with the high-level QCISD(T) results. The results of the semiempirical density functional computations also agree quite well with these highly correlated *ab initio* data. While the differences between the correlated PMP4 level and the HF level are relatively small, very significant quantitative and even qualitative differences occur; however, if either spin contaminations are annihilated or electron correlation effects are included *in the absence of accounting for the other effect*. After a discussion of some characteristics of the profiles shown in Figure 5, a few instructive cases will be cited to highlight the methodological differences.

At the HF level, activation barriers of 10.1 and 5.0 kcal/mol are found for the processes **1a** ⇒ **4a**‡ and **1b** ⇒ **4b**‡, respectively. The rotational barrier are *slightly* reduced after annihilation of spin contamination and accounting for electron correlation effects. At the PMP4 level, the activation barriers for the processes **1a** ⇒ **4a**‡ and **1b** ⇒ **4b**‡ are 9.2 and 3.3 kcal/mol, respectively. This computed rotational barrier for **1a** is comparable to the activation barriers of 8–14 kcal/mol measured for some disubstituted systems $[RC(SR)_2]^+$.[7] For the automerizations **2a** ⇒ **5a-u**‡ ⇒ **2a** and **2a** ⇒ **5a-w**‡ ⇒ **2a**, the activation barriers are 8.5 and 7.8 kcal/mol, respectively, at the highest level. For the automerizations of **2b** via **5b-u**‡ or **5b-w**‡, the activation barriers are 4.7 and 7.8 Kcal/mol, respectively. One would have expected that the rotational processes in the dication are less hindered than in the monocation and this is true for the isomerizations via **4** and for most automerizations but not for the automerization via **5b-w**‡. The automerization of **1** involves a sequence of isomerizations to **2** via **4**‡ and automerizations of **2** via **5**‡,

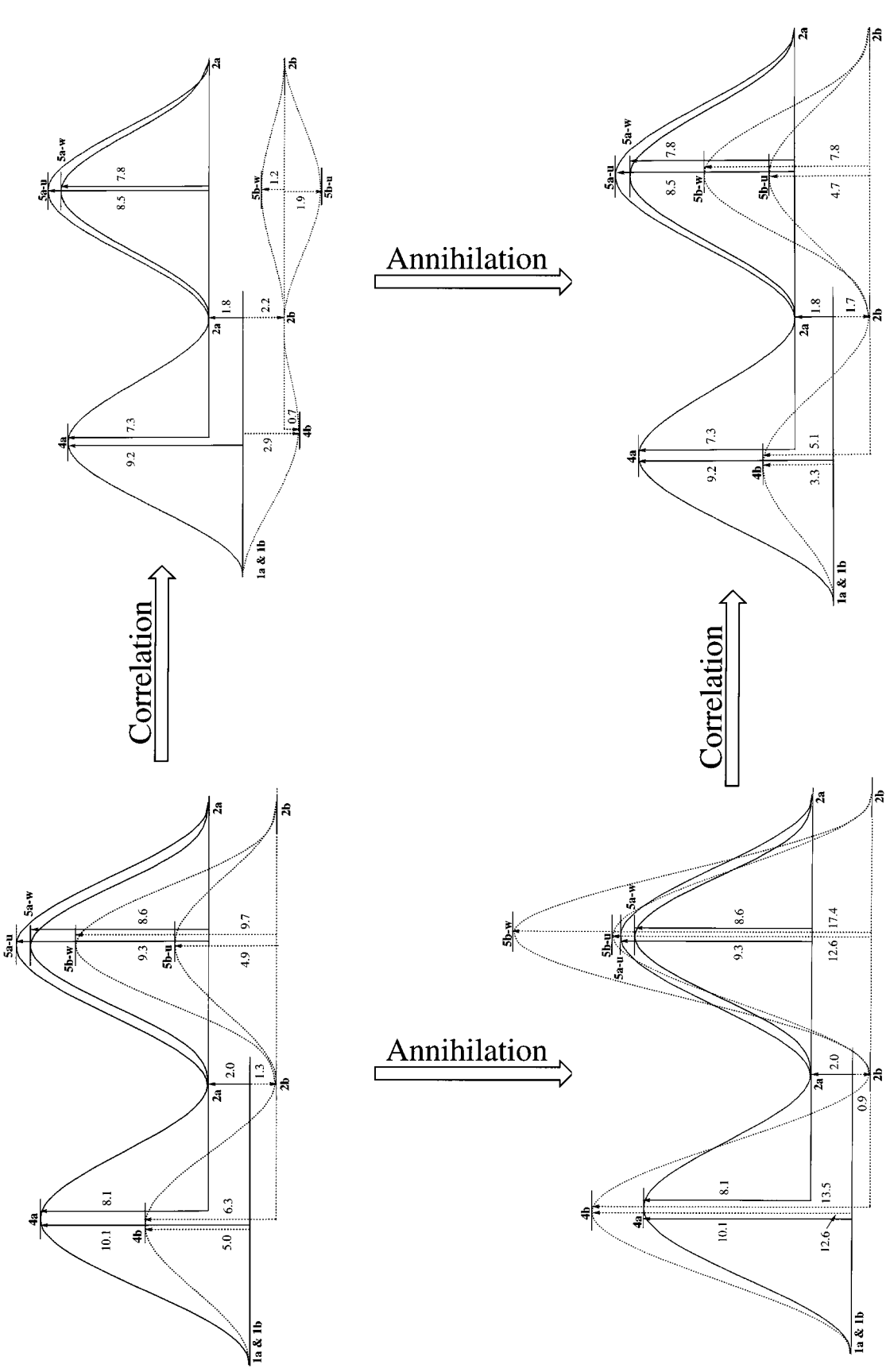

FIGURE 5. Schematic and to scale potential energy surface diagram are shown for the (—) monocation and (---) the dication radical. On the top left the potential energy diagram is represented to scale as computed at the HF/6–31G* + ΔVZPE level and the energetic consequences of either annihilation of spin contamination or electron correlation are shown in lower left and upper right corners, respectively. Both annihilation and electron correlation are considered at the PMP4/6–31G*//HF/6–31G* + ΔVZPE level shown on the lower right.

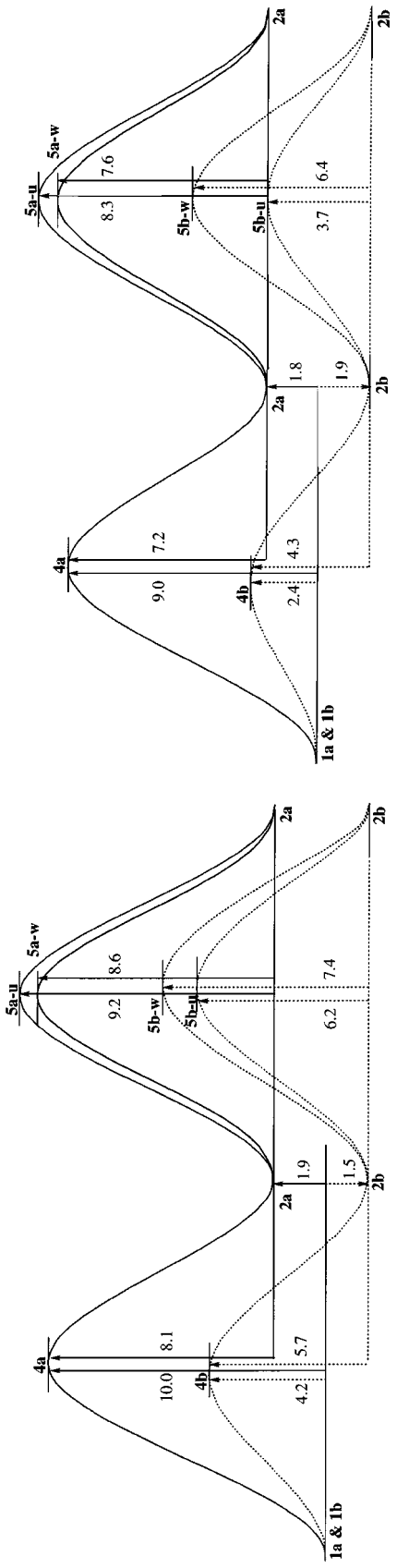

FIGURE 6. Density functional theory, B3LYP, and high level quadratic CI theory, QCISD(T), both agree very well with the scenario predicted at the PMP4 level. As in Figure 5, the potential energy diagram computed at the B3LYP/6−31G*//HF/6−31G* + ΔVZPE(HF/6−31G*) level is represented on the left and the QCISD(T)/6−31G*//HF/6−31G* + ΔVZPE(HF/6−31G*) data are depicted on the right.

and the former isomerizations are rate limiting for the monocation while the latter is rate limiting for the dication.

To illustrate the energetic effects of spin projection and electron correlation, a consideration of the automerization of **2b** via **5b-u** is particularly instructive. For the processes **2a** ⇒ **5a-u**‡ ⇒ **2a** and **2b** ⇒ **5b-u**‡ ⇒ **2b**, the activation barriers are 9.3 and 4.9 kcal/mol, respectively, at the HF level and the respective PMP4 barriers are similar (*vide supra*). Although **5b-u** is a transition state structure on the UHF potential energy surface, the MP4 energies calculated with the spin-contaminated UHF reference wave function would suggest that **5b-u** is more stable than **2b.** The MP2 level rotational profile of benzyl radical presents a similar case of such an artificial negative rotational barrier scenario.[30] With the data in Table IV we can trace the origin of this artifact. **2b** is spin contaminated substantially, and more so than **5b-u**, and the removal of these spin contaminants increases E_A(**2b** ⇒ **5b-u**) from 5.0 to 12.7 kcal/mol primarily because **2b** is stabilized by projection more than **5b-u** (ΔE_1 and ΔE_2 in Table III). On the other hand, electron correlation effects stabilize **5b-u** more than **2b**, counteracting the energetic effects of spin projection, and a PMP4 value results for E_A(**2b** ⇒ **5b-u**) that is close to the UHF value. The MP4 energies calculated without spin projection also indicate a reduction of E_A(**2b** ⇒ **5b-u**); but because spin annihilation, which increases E_A, is not properly accounted for, the resulting value of E_A(**2b** ⇒ **5b-u**) = −1.78 is much too low and would even suggest a change in the characteristics of the potential energy surface. This example well illustrates that MP perturbation theory, even when carried to full fourth-order, does not eliminate the spin contamination of the UHF reference and that PMP4 theory is required in such a case. Similar discussions apply to the activation barriers for the automerization **2b** ⇒ **5b-w** and the isomerization **1b** ⇒ **4b** ⇒ **2b**.

Conclusion

Spin polarization and dynamic electron correlation are both important for the radical dication $[C(SH)_3]^{\cdot,2+}$. MO diagram analysis reveals the readily identifiable feature responsible for these effects. Removal of an electron from one of the degenerate π HOMOs of C_{3h} symmetric $[C(SH)_3]^+$ results in a stabilization of the remaining π electron to such an extent that the unpaired electron is

not in the HOMO of the dication. The ''diving below the Fermi level'' of the unpaired π electron facilitates strong spin polarization because of the energetic proximity with σ MOs. The combination of annihilation of spin contamination and electron correlation is essential for the determination of relative energies and rotational barriers and affords an accuracy that matches the QCISD(T) results in a near-quantitative fashion. Importantly, pertubation theory alone does not correct for spin contamination even if it is carried to full fourth-order and includes triple excitations; the ΔE_3 values are all negative and can exceed 5 kcal/mol in magnitude. Previous studies showed that annihilation of spin contaminations is important in regions of potential energy surfaces where σ bonds are broken (homolytic dissociation), formed (radical addition), or both (H abstraction by radical). The results presented here stress that the annihilation of spin contaminations can be just as important for any process that greatly alters spin polarization and even if that process proceeds without breaking or forming of σ bonds.

Acknowledgments

This research was supported by a NATO Collaborative Research Grant. We thank the MU Campus Computing Center for generous allocations of computer time and Hossein Tahani for his assistance.

References

1. Reviews: (a) G. A. Olah and A. M. White, *Chem. Rev.*, **70**, 561 (1970); (b) C. U. Pittman, Jr., S. P. McManus, and J. W. Larsen, *Chem. Rev.*, **72**, 357 (1972); (c) M. Sundaralingam and A. K. Chwang, In *Carbonium Ions*, vol. 5 G. A. Olah and P. v. R. Schleyer, Eds., Wiley, New York, 1976, p 2457; (d) G. A. Olah, *Angew. Chem. Int. Ed. Engl.*, **32**, 767 (1993).
2. L. C. Allen, *J. Am. Chem. Soc.*, **111**, 9003 (1989).
3. See for example: (a) T. Okayama, In *Review of Heteroatom Chemistry*, vol. 1, S. Oae, Ed., MYU, Tokyo, 1988, p. 46; (b) P. K. Claus, In *Methods of Organic Chemistry*. Houben–Weyl–Müller, Eds, vol. 11, Part 2, Thieme Verlag, Stuttgart, Germany, 1985, p. 1469; (c) W. P. Tucker and L. P. Glenn, *Tetrahedron Lett.*, **29**, 2747 (1967); (d) I. Stahl and I. Kuehn, *Chem. Ber.*, **116**, 1739 (1983); (e) M. Frasch, S. Mono, H. Pritzkow, and W. Sundermeyer, *Chem. Ber.*, **126**, 273 (1993).
4. R. Gompper and E. Kutter, *Chem. Ber.*, **98**, 1365 (1965).
5. W. P. Tucker and G. L. Roof, *Tetrahedron Lett.*, 2747 (1967).
6. (a) G. A. Olah, A. Ku, and A. M. White, *J. Org. Chem.*, **34**, 1827 (1969); (b) G. A. Olah and A. M. White, *J. Am. Chem. Soc.*, **90**, 6087 (1968).
7. L. Hevesi, S. Deasauvage, B. Georges, G. Evrad, O. Blanpain, A. Michel, S. Harkema, and G. J. van Hummel, *J. Am. Chem. Soc.*, **106**, 3784 (1984).
8. L. O. Atovmyan and V. I. Ponomarev, *Zh. Strukt. Khim.*, **16**, 920 (1975).
9. D. Ohlmann, C. M. Marchand, H. Grützmacher, G. S. Chen, D. Farmer, R. Glaser, A. Currao, R. Nesper, and H. Pritzkow, *Angew. Chem. Int. Ed. Engl.*, **35**, 300 (1996).
10. R. Glaser, G. S.-C. Choy, G. S. Chen, and H. Grützmacher, *J. Am. Chem. Soc.*, **118**, 11617 (1996).
11. (a) V. Ferretti, V. Bertolasi, P. Gilli, and G. Gilli, *J. Phys. Chem.*, **97**, 13568 (1993); (b) K. B. Wiberg and K. E. Laidig, *J. Am. Chem. Soc.*, **109**, 5935 (1987).
12. H. B. Schlegel, *J. Chem. Phys.*, **84**, 4530 (1986).
13. H. B. Schlegel, *J. Phys. Chem.*, **92**, 3075 (1988).
14. J. J. W. McDouall and H. B. Schlegel, *J. Chem. Phys.*, **90**, 2363 (1989).
15. C. Sosa and H. B. Schlegel, *J. Am. Chem. Soc.*, **109**, 4193 (1987).
16. (a) C. Sosa and H. B. Schlegel, *Int. J. Quantum Chem.*, **29**, 1001 (1986); (b) C. Sosa and H. B. Schlegel, *Int. J. Quantum Chem.*, **30**, 155 (1986).
17. C. Gonzalez, C. Sosa, and H. B. Schlegel, *J. Phys. Chem.*, **93**, 2435 (1989).
18. J. R. Alvarez–Idaboy, L. A. Eriksson, T. Fängström, and S. Lunell, *J. Phys. Chem.*, **97**, 12737 (1993).
19. R. Arnaud, H. Postlethwaite, and V. Barone, *J. Phys. Chem.*, **98**, 5913 (1994).
20. W. H. Donoan and G. R. Famini, *J. Phys. Chem.*, **98**, 7811 (1994).
21. M. W. Wong and L. Radom, *J. Phys. Chem.*, **99**, 8582 (1995).
22. C. Gonzalez, J. J. W. McDouall, and H. B. Schlegel, *J. Phys. Chem.*, **94**, 7467 (1990).
23. J. S. Francisco, *J. Chem. Phys.*, **96**, 7597 (1992).
24. (a) J. C. Corchado, F. J. Olivares del Valle, and J. Espinosa–Garcia, *J. Phys. Chem.*, **97**, 9129 (1993); (b) J. Espinosa–Garcia, E. A. Ojalvo, and J. C. Corchado, *J. Mol. Struct.* (*Theochem.*), **303**, 131 (1994).
25. S. Sekusak, H. Güsten, and A. Sabljic, *J. Chem. Phys.*, **102**, 7504 (1995).
26. C. Gonzalez and H. B. Schlegel, *J. Am. Chem. Soc.*, **114**, 9118 (1992).
27. R. D. Bach, H. B. Schlegel, J. L. Andrés, and C. Sosa, *J. Am. Chem. Soc.*, **116**, 3475 (1994).
28. (a) R. Glaser and G. S.-C. Choy, *J. Phys. Chem.*, **97**, 3188 (1993); (b) R. Glaser and G. S.-C. Choy, *J. Phys. Chem.*, **98**, 11379 (1994).
29. K. B. Wiberg, J. R. Cheeseman, J. W. Ochterski, and M. J. Frisch, *J. Am. Chem. Soc.*, **117**, 6535 (1995).
30. D. A. Horvat and W. T. Borden, *J. Phys. Chem.*, **98**, 10460 (1994).
31. W. T. Borden and R. E. Davidson, *Acc. Chem. Res.*, **29**, 67 (1996).
32. J. A. Pople and R. K. Nesbet, *J. Chem. Phys.*, **22**, 571 (1954).
33. J. I. Musher, *Chem. Phys. Lett.*, **7**, 397 (1970) and references cited therein.
34. P. O. Löwdin, *Quantum Theory of Atoms, Molecules, and the Solid State*, Academic Press, New York, 1966, p. 601.
35. Review: M. Karplus and P. J. Rossky, *J. Chem. Phys.*, **73**, 6196 (1980).

36. H. Nakatsuji, H. Kato, and T. Yonezawa, *J. Chem. Phys.*, **51**, 3175 (1969).
37. W. J. Hehre, L. Radom, P. v. R. Schleyer, and J. A. Pople, *Ab Initio Molecular Orbital Theory*, Wiley, New York, 1986.
38. P. J. Knowles and N. C. Handy, *J. Phys. Chem.*, **92**, 3097 (1988).
39. (a) R. J. Bartlett, J. F. Stanton, In *Reviews of Computational Chemistry*, vol. 5, K. B. Lipkowitz and D. B. Boyd, Eds., VCH, New York, 1994, p. 65; (b) J. A. Pople, M. Head−Gordon, and K. Raghavachari, *J. Phys. Chem.*, **87**, 5968 (1987).
40. (a) L. J. Bartolotti, K. Flurchick, in *Reviews of Computational Chemistry*, vol. 7, K. B. Lipkowitz and D. B. Boyd, Eds., VCH, New York, 1996, p. 187; (b) N. H. March, *Electron Density Theory of Atoms and Molecules*, Academic Press, Inc., San Diego, CA, 1992; (c) J. K. Labanowski and J. W. Andzelm, Eds., *Density Functional Methods in Chemistry*, Springer−Verlag, New York, 1992; (d) R. G. Parr and W. Yang, *Functional Theory of Atoms and Molecules*, Oxford University Press, New York, 1989.
41. (a) A. D. Becke, *Phys. Rev. A*, **33**, 2786 (1986); (b) A. D. Becke, *J. Chem. Phys.*, **88**, 2547 (1988); (c) C. Lee, W. Yang, and R. G. Parr, *Phys. Rev. B*, **37**, 785 (1988).
42. P. O. Löwdin, *Phys. Rev.*, **97**, 1509 (1955).
43. (a) W. Chen and H. B. Schlegel, *J. Chem. Phys.*, **101**, 5957 (1994); (b) See refs. 12−14.
44. M. J. Frisch, G. W. Trucks, H. B. Schlegel, P. M. W. Gill, B. G. Johnson, M. A. Robb, J. R. Cheeseman, T. Keith, G. A. Peterson, J. A. Montgomery, K. Raghavachari, M. A. Al-Laham, V. G. Zakrzewski, J. V. Ortiz, J. B. Foresman, J. Cioslowsky, B. B. Stefanov, A. Nanayakkara, M. Challacombe, C. Y. Peng, P. Y. Ayala, W. Chen, M. W. Wong, J. L. Andres, E. S. Replogle, R. Gomperts, R. L. Martin, D. J. Fox, J. S. Binkley, D. J. Defrees, J. Baker, J. J. P. Stewart, M. Head−Gordon, C. Gonzalez, and J. A. Pople, Gaussian 94, *Revision C.3*, Gaussian, Inc., Pittsburgh, PA, 1995.
45. The situation is closely related to $(H_2C)_3C^{\cdot+}$ and $C_6H_6^{\cdot+}$: (a) Trimethylene methane radical cation: P. Du and W. T. Borden, *J. Am. Chem. Soc.*, **109**, 5330 (1987); (b) Benzene cation is D_{2d} symmetric but fluctional and best viewed as D_{6h} symmetric: R. Lindner, K. Müller−Dethlefs, E. Wedrum, K. Haber, and E. R. Grant, *Science*, **271**, 1698 (1996).